Architecture at the Mesoscale: Morphogenesis of Novel Patterned Alkaline Earth Containing Mesoporous Silica

Constantinos C. Pantazis,* Alexandros P. Katsoulidis, and Philippos J. Pomonis

Department of Chemistry University of Ioannina, Ioannina 45110, Greece

Received July 4, 2005. Revised Manuscript Received October 20, 2005

We report the synthesis of alkaline earth induced/containing complex constructions of mesoscale mesoporous silica particles with novel patterned surfaces and controllable porosity and morphology by employing a poly(acrylic acid)−cetyltrimethylammonium bromide complex template. The addition of the alkaline earth metals Mg or Sr induced the morphosynthesis of some fascinating curved particles exhibiting complex discoid and gyroid morphologies with novel patterned surfaces of increased complexity consisting of platelike fins or regular creased coronas. The use of Ca results in ordinary particles without long-range morphology. The uncalcined materials possess long-range hexagonal ordering, while upon calcination the respective loss of order does not affect the particular morphology. The materials are synthesized and preserve their intrinsic characteristics in a wide range of pH values extending from 5.5 to 9.0. The morphology, the porosity, and the metal concentration of the particles are affected and can be controlled by the pH. Increase of the latter favors the transformation from discoid with peripheral platelike fins to gyroid particles with creased, thick coronas in the case of Sr, while for the case of Mg at pH 9.0 the gyroids embody either discoids with peripheral platelike fins or patterned coronas. At the lower pH the materials are microporous. When the pH is increased, mesoporous materials are obtained. In this way porosity is controlled by a simple variation of pH, without the use of surfactants with longer chains. The amount of metal on the mesostructure is also increased with the pH.

Introduction

Mesoscale chemistry embodying the concepts of morphosynthesis, defect design, and biomimetics[1−5] emerges as a powerful tool for the rational design of new hierarchical, functional materials. The ability to sculpture particular morphological characteristics on the mesoscale particles, a process nature handles with great efficiency, is sought by the material scientists as it opens new ways for separation, catalysis, nanoelectronics, and energy technologies.

At the same time, being able to induce new physical or chemical properties, by incorporation of metals (basicity/acidity) or efficient control of porosity of the mesoscale particles (micro-/mesoporosity) targeting a specific application, would be desirable. However, biomimetic morphosynthesis has so far been focused mainly on pure silica. A wide variety of patterns and forms of mesoscale particles have been developed by making use of either biomimetic silicification employing various biomolecules or polyelectrolyte systems[6−8] or by common template systems employing surfactants of the alkyl-trimethylammonium type[9−14] in highly acidic conditions, which do not favor incorporation of a high amount of metals in the mesostructure.

The obtained morphologies include fibers, toroids, and spheres as well as discoids, spiral shapes, and gyroids with smooth or radially patterned surfaces. Such radial patterns on discoid or gyroid particle surfaces are the only ones observed so far.

In this work we exploit ionic self-assembly and, specifically, poly(acrylic acid) (molecular weight, MW, 2000 g mol^{-1}; Pac2)−cetyltrimethylammonium bromide (CTAB) complexes as the template. Polyelectrolyte−surfactant complexes have been known for quite some time as a new type of highly ordered mesomorphous *organic* solids,[15−17] and their potential, as building blocks, in the synthesis of functional nanostructured materials has early been identified.[18,19] Their formation follows a highly cooperative zipper mechanism under a stoichiometry of 1:1, driven by Cou-

* To whom correspondence should be addressed. Fax: +32651098795. E-mail: me00596@cc.uoi.gr.

(1) Antonietti, M.; Ozin, G. A. *Chem.—Eur. J.* **2004**, *10*, 28.
(2) Ozin, G. A. *Acc. Chem. Res.* **1997**, *30*, 17.
(3) Mann, S.; Ozin, G. A. *Nature* **1996**, *382*, 313.
(4) Dujardin, E.; Mann, S. *Adv. Eng. Mater.* **2002**, *4*, 461.
(5) Yang, H.; Ozin, G.; Kresge, C. *Adv. Mater.* **1998**, *10*, 883.
(6) Po Foo, C. W.; Huang, J.; Kaplan, D. L. *Trends Biotechnol.* **2004**, *22*, 577.
(7) Patwardhan, S. V.; Clarson, S. J.; Perry, C. C. *Chem. Commun.* **2005**, *9*, 1113.
(8) Sun, Q.; Vrieling, E. G.; van Santen, R. A.; Sommerdijk, N. A. J. M. *Curr. Opin. Solid State Mater. Sci.* **2004**, *8*, 111.
(9) Yang, H.; Coombs, N.; Ozin, G. *Nature* **1997**, *386*, 692.
(10) Ozin, G. A. *Can. J. Chem.* **1999**, *77*, 2001.
(11) Sokolof, I.; Yang, H.; Ozin, G.; Kresge, C. *Adv. Mater.* **1999**, *11*, 636.
(12) Wang, B.; Shan, W.; Zhang, Y.; Xia, J.; Yang, W.; Gao, Z.; Tang, Y. *Adv. Mater.* **2005**, *17*, 578−581.
(13) Lin, H. P.; Mou, C. Y. *Acc. Chem. Res.* **2002**, *35*, 927.
(14) Yang, S. M.; Yang, H.; Coombs, N.; Sokolof, I.; Kresge, C.; Ozin, G. *Adv. Mater.* **1999**, *11*, 52.
(15) Antonietti, M.; Conrad, J. *Angew. Chem., Int. Ed. Engl.* **1994**, *33*, 1869; *Angew. Chem.* **1994**, *106*, 1927.
(16) Antonietti, M.; Conrad, J.; Thuneman, A. *Macromolecules* **1994**, *27*, 6007.
(17) Hayagawa, K.; Santere, J. P.; Kwak, J. C. T. *Macromolecules* **1983**, *16*, 1642.
(18) Ober, C. K.; Wegner, G. *Adv. Mater.* **1997**, *9*, 17.
(19) Faul, C. F. J.; Antonietti, M. *Adv. Mater.* **2003**, *15*, 673.

10.1021/cm051450z CCC: $33.50
Published on Web 11/25/2005

Table 1. Structural Characteristics and Composition of the Corresponding Samples

sample code	phase (XRD)	d_{100}[a] (Å)	d_{100}[b] (Å)	HK[c] diameter (Å)	BET surface area ($m^2\ g^{-1}$)	% atomic[b] (with respect to Si atoms) Sr or Mg (EDS)
$Pac2C_{16}Mg$ 5.5	hexagonal	41.7	31.1	20	1131	1.2
$Pac2C_{16}Mg$ 7.5	hexagonal	42.1	36.5	31	1103	3.1
$Pac2C_{16}Mg$ 9.0	hexagonal	42.3	36.7	29	915	3.4
$Pac2C_{16}Sr$ 5.5	hexagonal	40.2	36.8	20	945	2.3
$Pac2C_{16}Sr$ 7.5	hexagonal	41.5	40.3	27	990	4.4
$Pac2C_{16}Sr$ 9.0	hexagonal	41.8	41.2	25	992	2.5

[a] Refers to the uncalcined samples. [b] Refers to the calcined at 600 °C samples. [c] The psd was calculated according to the Horvath−Kawazoe (HK) method.

lombic interactions between the functional groups of the anionic polyelectrolyte backbone and the cationic surfactant as well as hydrophobic interactions among the surfactant chains.

We first used these complexes as template systems in the presence of a silica source (tetraethyl orthosilicate, TEOS) for the preparation of pure and copper containing hexagonal as well as pure cubic *Pm*3*n* mesoporous silica.[20−22] However, the materials did not bare any particular morphology other than hexagonal-like or spherical particles, common in the synthesis of template assisted hexagonal or cubic mesoporous silica. In an attempt to affect the development of the template we proceeded in a first approach to the addition of alkaline earths such as Mg, Ca, and Sr, which are the most frequently met in natural hierarchical morphogenetic systems.[25]

In the subject system, Pac can act as a carrier of the metal cations, via complexation onto its chain, into the developing hybrid mesophase. This interference of the cations in the complexation process of Pac with CTAB, which is responsible for the complex template formation,[20−22] is likely to cause topological defects in the evolving mesophase that could orchestrate a morphological shaping at the mesoscale. However, that effect should be influenced by the particular metal cation as the complexation properties are differentiated for each metal. Additionally, the complexation process leads to high dispersion of the metals on the mesostructure.[22]

Experimental Section

Synthesis Protocol. At ambient temperature 0.70 g of poly(acrylic acid) (Aldrich) of MW 2000 g mol^{-1} was dissolved in 100 g of water under stirring. The pH of the solution, measured online, was typically pH ≈ 3.2. HCl acid is then used to set the pH at 1.5. Then C_{16}TAB (Merck) is added at a stoichiometric amount with respect to polyelectrolyte functional groups (3.58 g). After this addition a clear solution was obtained. Finally, 6 mL of TEOS (Merck) and 0.62 g of $SrNO_3$, 0.43 g of $CaCl_2{\cdot}2H_2O$, or 0.75 g of $MgNO_3{\cdot}6H_2O$ were introduced into the mixture so Si/M = 9, where M = Sr, Ca, or Mg. The molar composition of the mixture was TEOS/Pac2/C_{16}TAB/M/H_2O = 1:0.013:0.37:0.11:209 (where M = $SrNO_3$, $CaCl_2{\cdot}2H_2O$, or $MgNO_3{\cdot}6H_2O$).

Then a slow dropwise addition of 0.1 M NaOH with a constant rate of 0.5 mL min^{-1} started taking place under constant vigorous stirring for about 4 h. Intermediate samples were isolated at any desired pH, which was followed and recorded via a pHmeter during the process. The process of increase of pH leads eventually to precipitation of a white solid, visible at pH 3.2−3.5. Precipitates at the final pH 5.5, 7.5, or 9.0 were left for 24 h in the mixture. The samples are then subject to filtration, drying at 90 °C [T_g = 106 °C for poly(acrylic acid)], and calcination at 600 °C for 2 h with a heating rate 3 °C min^{-1} under atmospheric conditions.

Instrumentation and Characterization. Nitrogen adsorption measurements were performed at 77 K on a Sorptomatic 1990 Fisons Instrument after outgassing for 12 h at 473 K. X-ray diffraction measurements were acquired on a Bruker Advance D8 system using Cu Kα radiation (λ = 1.5418 Å) with a resolution of 0.01°. Scanning electron microscopy (SEM) was performed on a JEOL JSM 5600 at 20 kV equipped with an Oxford energy-dispersive spectroscopy (EDS) X-ray microanalysis apparatus.

Results and Discussion

Table 1 includes the structural and compositional characteristics of both the $Pac2C_{16}Mg$ and the $Pac2C_{16}Sr$ samples. The X-ray diffractograms of the corresponding samples are shown in Figure 1. All the obtained uncalcined samples possess hexagonal ordering, while calcination at 600 °C results in loss of order as indicated by the disappearance of the higher order Bragg peaks (110, 200, and 210).

The adsorption−desorption isotherms are shown in Figure 2. All samples possess high specific surface area ranging from 900 to 1100 $m^2\ g^{-1}$ and a pore size from 2 to 3 nm. For the two series of materials we observe significant differences in the shape of the isotherms as the pH increases. At pH 5.5 both materials exhibit a type-I adsorption isotherm typical of microporous systems with a pore diameter of 2 nm. As the pH is increased at 7.5 and 9.0, the development of mesoporosity is evident from the quite broad condensation step at P/P_0 = 0.3−0.4 of the adsorption isotherms, with a simultaneous appearance of a hysteresis loop of the desorption isotherm, which is more intensively observed in the case of Mg containing samples. This fact indicates the existence of a mesoporous network of a relevantly broad psd, as observed in the corresponding pore size distribution (psd) diagrams in Figure 2, as well as higher connectivity, reflecting the relatively low degree of order of the materials as also indicated by the X-ray diagrams of the calcined samples mentioned above. We should note that the difference of the d_{100} spacings between the uncalcined and calcined samples decreases as the pH increases from 5.5 to 7.5 and 9.0. This fact indicates lower contraction of the mesostructure

(20) Pantazis, C. C.; Trikalitis, P. N.; Pomonis, P. J.; Hudson, M. J. *Microporous Mesoporous Mater.* **2003**, *66*, 37.
(21) Pantazis, C. C.; Pomonis, P. J. *Chem. Mater.* **2003**, *15*, 2299.
(22) Pantazis, C. C.; Trikalitis, P. N.; Pomonis, P. J. *J. Phys. Chem. B* **2005**, *109*, 12574.
(23) Iler, R. K. *The Chemistry of Silica: Solubility, polymerization, colloid and surface properties and biochemistry*; Wiley: New York, 1979.
(24) Baes, C. F.; Mesmer, R. E. *The Hydrolysis of Cations*; Krieger: Malabar, FL, 1986.
(25) Mann, S. *Biominealization Principles and Concepts in Bioinorganic Materials Chemistry*; Oxford University Press: New York, 2001.

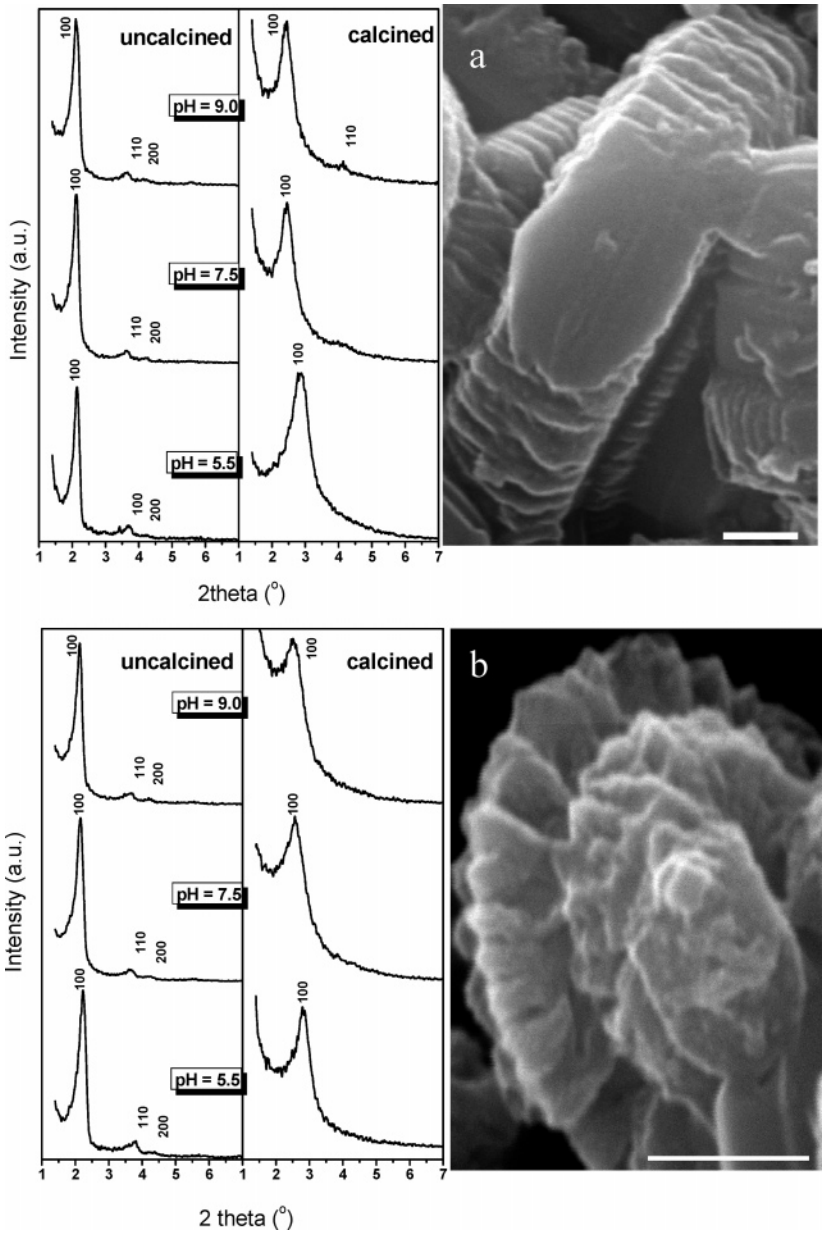

Figure 1. X-ray diffractograms of the uncalcined and calcined Pac2C_{16}Mg (a) and Pac2C_{16}Sr (b) samples at the pH values 5.5, 7.5, and 9.0 as indicated. The diagrams of the sample Pac2C_{16}Mg are accompanied with an image of a propellerlike gyroid particle synthesized at pH = 9.0 and the diagrams of the sample Pac2C_{16}Sr with a similar particle synthesized at pH = 5.5. Scale bar at 1 μm.

or higher thermal stability at increased pH that is probably a result of the higher condensation degree of silicon atoms.[23]

The amount of the corresponding metal is also increased with the pH. Considering that within the working pH range 5.5−9.0 the metal compounds of the Mg(II) and Sr(II) cations are soluble and do not precipitate[24] the increase of their concentration in the mesostructure with the pH should be due to complexation with the carboxylic groups of the poly(acrylic acid). However, pH values higher than 7.5, where all the carboxylic groups are ionized, should not lead to further increase of metals on the mesostructure if they were only carried through complexation with Pac. This is suggested by the corresponding values in Table 1, where for the case of Sr we observe a decrease of the metal amount at pH 9.0 compared with the highest value at pH 7.5. Finally, we should note that the total amount of metal on the mesostructure (2−4 mol %) is lower than that initially intended (10 mol %). This is presumably due to the occupation of the majority of the complexation sites of the polyelectrolyte with the cationic surfactant molecules that may also have a higher complex formation constant than the corresponding one of the metals.

The shapes of the particles of the sample containing Mg (Pac2C_{16}Mg) synthesized at the pH value 5.5 are depicted on Figure 3 (images a and b). They are all well -organized systems in the mesoscale regime. In the first image, image a, we observe a discoid particle which has developed an unusual, patterned surface consisting of remarkably regular creases in about five ellipsoidal crowns grown in a concentric way. Moreover, the thickness and size of the creases differ as we move to the center. The central oval consists of creases that are thicker, more attached to each other, and compressed at the edges, the regions of higher curvature. This pattern implies that the discoid has been developed by a $+2\pi$ disclination defect.[5] The formation of the creased surface, whose development was probably synchronized with that of

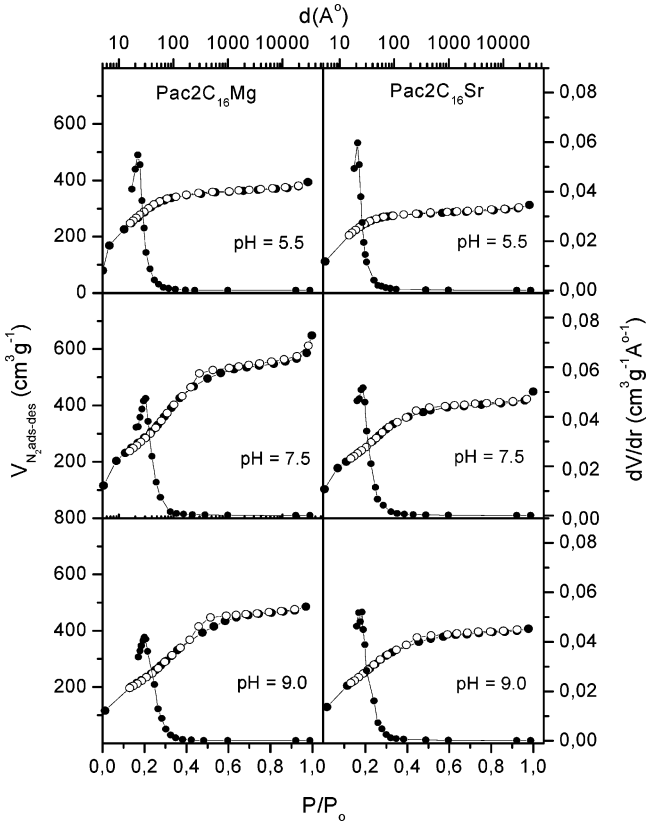

Figure 2. N_2 adsorption−desorption isotherms at 77 K for the Pac2C_{16}Sr (right) and Pac2C_{16}Mg (left) solids at the pH values indicated as well as corresponding psd's calculated according to the Horvath−Kawazoe method.

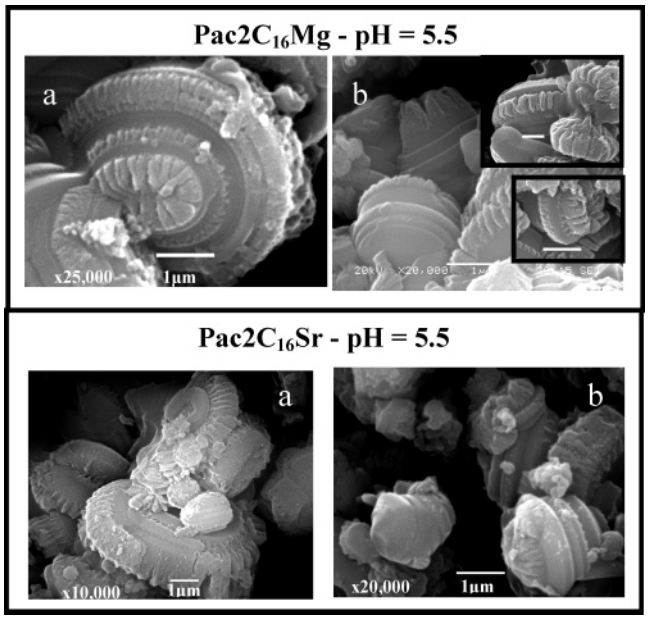

Figure 3. Representative SEM images of the calcined sample Pac2C_{16}Mg (upper image a) and uncalcined (image b and insets) as well as calcined sample Pac2C_{16}Sr (lower images a and b) at pH = 5.5. Scale bar is 1 μm in all inset images.

the discoid, could arise from a complex combination of topological defects and contraction stresses on the evolving silicatropic mesophase, induced by condensation and rigidification of the framework[11,14] in combination with the complexation of the metals.

Image b and the insets present discoid particles of the same uncalcined sample with similarly patterned surfaces. There we additionally observe that the creases may also surround peripherally the discoid, which is transformed into a propellerlike particle (upper inset image in part b). A magnification of a similar particle, which interestingly seems to be a complex construction of a gyroid that has developed a discoid propellerlike corona, may be better appreciated in Figure 1a. There, the 2 μm long fins have been regularly developed in even distances among each other and vertically to the surface of the body of the particle.

At this point we should emphasize that the materials developed in the presence of Ca did not exhibit perfected particle shapes as above but provided ordinary, undecorated particles of the same size, lacking any interesting morphological characteristics. A reason for this will be given in the following section of the mechanistic aspects regarding the development of the morphosynthetic particles.

On the contrary, the use of Sr results mostly in discoid particles decorated with peripheral fins or coronas as observed for the calcined sample Pac2C_{16}Sr, synthesized at the pH value 5.5. An image (image a) of this sample is shown in the lower part of Figure 3 as well as in Figure 1b, where a magnified similar particle with radially developed fins is seen. Very interestingly in image b of Figure 3, we recognize two similar constructions that do not seem to have developed via a $+\pi$ screw dislocation, but they rather consist of discoids with increasing diameters that are placed upon each other. Such structures pinpoint the possibility of a hierarchical construction ability of the system.

The particles of the sample containing Mg (Pac2C_{16}Mg) synthesized at pH 7.5 are depicted in Figure 4 (image a). They are gyroid particles with a smooth peripheral decoration of small creases near the base as well as on the top. This morphology is maintained at higher pH 9.0 as shown in image b and the inset of the upper part of Figure 4. Very interestingly, in image b we observe two "open" morphologies that probably represent intermediate stages of gyroid particle formation. It is very likely that the gyroid morphology emerges from a discoidal organization of hybrid micelles with creased periphery, whose edges bend toward each other. When the edges meet, diffusion and growth could lead to the final complex gyroid morphology.

In the lower part of Figure 4, images of the samples containing Sr (Pac2C_{16}Sr), synthesized at pH 7.5 (images a and b) and 9.0 (images c and d), are shown. The inset image in image b of Figure 4 shows a fully decorated gyroid in fine detail developed at pH 7.5. As the pH increases from 5.5 (lower part of Figure 3, images a and b) to 9.0, the particles seem to gradually adopt a gyroid morphology consisting of intensively creased surfaces.

Mechanistic Aspects of Mesoscale Particle Formation. The morphologies obtained from similar template systems that make use of cationic surfactants in acidic conditions and include fibers, toroids, and spheres as well as discoids, spiral shapes, and gyroids with smooth or radially patterned surfaces are believed to be initiated by an elastically deformable hybrid nucleus (seed) of 50 nm in size. Its sustainable growth and shape depends on the interplay of colloidal interactions with the hybrid micelles determined by the synthesis conditions—ionic strength, pH, dielectric

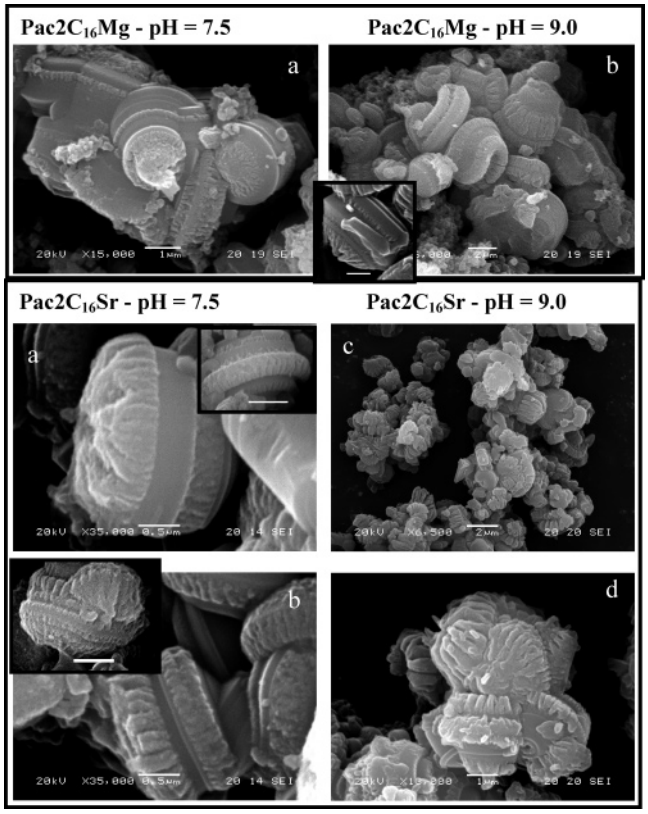

Figure 4. Upper part: representative SEM images of the calcined sample $Pac2C_{16}Mg$ at pH = 7.5 and 9.0 (images a and b, respectively) and uncalcined at pH = 9.0 (inset image in b). Lower part: representative SEM images of the calcined sample $Pac2C_{16}Sr$ at pH = 7.5 (images a, b, and insets), at pH = 9.0 (image c) and uncalcined at pH = 9.0 (image d). Scale bar is 1 μm in all inset images.

constant, and temperature—and elastic forces. This interplay brings about topological defects that force the developing nanomesophase to adopt a certain shape that eventually determines the final particle morphology.

The key factor of the subject system is the pH, which affects/controls the following procedures that evolve simultaneously: (i) complexation of the cationic surfactant with Pac, that is, the evolution of the template mesophase, (ii) the degree of complexation of the metals with the carboxylic groups of the polyelectrolyte, (iii) the growth and shape of the evolving nucleus, and (iv) the hydrolytic polycondensation of the silica precursor.

As the pH is increased during the synthesis process in a stepwise mode with a constant rate, the condensation rate of silica, the degree of Pac−C_nTAB complexation, and the degree of metal complexation constantly increase in return. These dynamic processes, which take place in the midst of the structural evolution and keep the developing system constantly out of equilibrium, should affect nucleation and growth rates as well as shape of the seed, in a specific, yet complex and unknown, way with a translational effect on the final particle morphology.

As a result of its intrinsic complexity some mechanistic aspects of the system will be mentioned in a first attempt to rationalize the development of the morphosynthetic particles, based on a combination of the data mentioned in the context of this work with those of relevant literature.

The formation of the particular particle morphology is realized only in the presence of the metals, which possibly implies that effects related to silica hydrolysis and condensation are not of crucial importance in the subject system. Although their presence could also induce an indirect effect to silica hydrolysis and condensation rates (e.g., increase of ionic strength), it is believed that a direct effect of them, steaming from their complexation with the poly(acrylic acid), is responsible for the observed morphologies.

Alkaline earth species show a relatively decreased tendency to suffer hydrolysis and precipitation. This tendency is further decreased in the order Mg >Ca > Sr and only above pH 9 the species $MgOH^+$ are becoming important.[24] This means that within the working pH range the hydrated cations are the predominant species.

Complexation of poly(acrylic acid)[26−29] and other carboxyl compounds such as modified polysaccharides[30] and resins[31] with alkaline earth metals has been investigated mainly for Mg and Ca. They form stable complexes with formation constants lying in the range 10^2-10^5 depending on the ionic strength, the pH, their concentration, the MW of the polyelectrolyte, and the medium.

Their formation constants follow the order Mg < Ca < Sr and are related to the size of the ions and their hydration efficiency, which follows the opposite order.[28,32] The main complexes formed in the subject system between poly(acrylic acid) and Mg or Ca considering their concentration in the reactant solution (30 mM) as well as the concentration of Pac (2.5 mM) and carboxylic groups (70 mM) are mainly MgL for Mg and CaL_2 for Ca,[26] where $L = COO^-$. It is also reasonable to assume formation of SrL_2 for Sr on the basis of the above.

Moreover, as the pH increases the complexes become more stable and their formation percentages increase with a maximum at pH around 8[27] depending also reversely on the ionic strength and analogously on the stability of the complex. Typically, at pH 8 and ionic strength 0.1 M, which is closer to our case, about 80 and 76% of Ca and Mg complex formation has taken place with formation constants $10^{5.34}$ and $10^{5.09}$, respectively.

As a conclusion, increase of pH leads to more stable complexes and increase of the degree of complexation, which is expected as the concentration of ionized carboxylic groups is increased in return.

In our system the concentration of Mg and Sr in the solids follows the same trends, with, however, lower values (about 30% of the initially added Mg and 40% of Sr were finally incorporated), which is expected as the rest of the functional groups are occupied by the cationic surfactant molecules.

Considering the above we can conclude with a mechanistic scheme for the development of the morphosynthetic particles.

(26) De Stefano, C.; Gianguzza, A.; Piazzese, D.; Sammartano, S. *Mar. Chem.* **2004**, *86*, 33.
(27) De Stefano, C.; Gianguzza, A.; Piazzese, D.; Sammartano, S. *Talanta* **2003**, *61*, 181.
(28) Ogawara, K.; Kawazoe, S.; Tamura, T.; Kawauchi, S.; Satoh, M.; Komiyara, J. *Polymer* **1998**, *39*, 437.
(29) Iida, S. *Biophys. Chem.* **1996**, *57*, 133.
(30) Crescenzi, V.; Dentini, M.; Meoli, C.; Casu, B.; Naggi, A.; Torri, G. *Int. J. Biol. Macromol.* **1984**, *6*, 142.
(31) Harju, L.; Krook, T. *Talanta* **1995**, *42*, 431.
(32) Abraham, T.; Kumpulainen, A.; Xu, Z.; Rutland, M.; Claesson, P. M.; Masliyah, J. *Langmuir* **2001**, *17*, 8321.

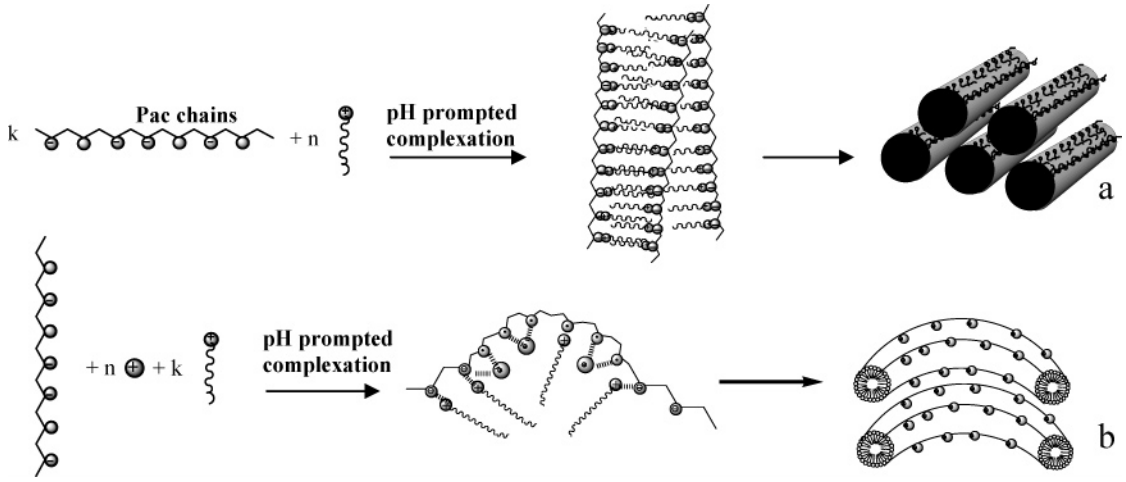

Figure 5. Possible bending of the polyelectrolyte chains caused by complexation of the alkaline earth cations with the carboxylic groups on the backbone of the former that could lead to curved micelles (b) in contrast to the case of the absence of metals in the reactant solution (a). The topological constant increase of curvature in the hybrid elastic mesophase is suggested to be able to generate the observed discoid and gyroid particles with the highly curved decoration patterns.

In the absence of the metals the system generates straight cylindrical micelles, which result to no particular particle morphology.[20,21] It is known that poly(acrylic acid) gradually adopts a stretched conformation with the increase of pH.[33] In the presence of the metals, complexation of the latter with poly(acrylic acid) functional groups is possible. The complexation is possible to cause the chain contraction of the polyelectrolyte as has been suggested for the system Pac/Ca,[28,29] whose extent and intension should depend on the complexation degree, which is increased with the pH and complexation strength, which is also increased from Mg to Sr as well as with increase of pH.

According to this line of thinking, the bended polyelectrolyte chains as a part of the combined micelle and mesophase formation, as has been described previously,[20] should lead to curved micelles that could generate discoid particles at low pH (images in Figure 3), which could be transformed at gyroid particles at higher pH (upper image in Figure 4b), where extensive curvature will have been induced by the higher concentration of the metals and the more stable metal complexes. Moreover, the constantly increased topological curvature, induced by the constant increase of the metals in the elastic hybrid mesophase, homogeneously spread on the particle bodies could lead to the highly curved decoration on them, which is culminated at the particles containing Sr at pH 9 (Figure 5).

Finally, we should make a comment for the absence of similar particles in the presence of Ca. In this work the use of $CaCl_2$ instead of $Ca(NO_3)_2$, that is, the Cl^- (about 60 mM) anions instead of the NO_3^- anions, could possibly inhibit the complexation of Ca with the carboxylic groups of the polyelectrolyte as the smaller Cl^- anions can stabilize more effectively the positive charge of the hydrated metal. This effect has been mentioned for the Ca/Pac system, where excessive addition of KCl (30−300 mM) inhibits the complexation process. The result should be weaker and lower the degree of complexation, which should not possibly be able to induce the required curvature to the developing micelles. In fact the atomic concentration of Ca at the solids isolated at pH 9 was 2%, about two times lower than expected.

Conclusions and Outlook

Concluding the above results, we were able to develop discoid and gyroid mesoscale, mesoporous silica particles, with patterned surfaces in the form of peripheral platelike fins and regular creases by employing a poly(acrylic acid)−CTAB complex template in the presence of Mg and Sr. Their significant role in the synthesis of these particular shapes is defined by the fact that the metal-free reaction system is incapable of inducing morphosynthesis. However, whether it is their existence on the mesostructure or a more subtle effect of them in the reactant mixture that leads to these novel morphologies remains to be answered. The particles appear in the whole optical field of the image baring various degrees of perfection. The system achieves at the same time morphosynthesis and metal introduction as the former necessitates the latter. Moreover, the porous structure, the metal concentration, and the morphology of the particles can be controlled by the simple variation of pH, depending also on the metal. The materials preserve their intrinsic characteristics in a wide range of pH values extending from 5.5 to 9.0. The physicochemical properties of the materials with respect to application in heterogeneous catalysis (biodiesel, methane reforming), the effect of other metals, and the possibility of manipulating a hierarchical construction ability of the system, after further research in the mechanistic pathways of the morphosynthetic particle development, are topics currently under investigation.

Acknowledgment. We acknowledge financial support from the Projects HERAKLEITOS and PYTHAGORAS from EU and the Ministry of Education (EPEAEK) as well as the Project PENED 2003 from EU and from the General Secretariat of Research and Technology (GSRT). We also acknowledge the valuable assistance from N. Kourkoumelis and the SEM and XRD units of the Network of Laboratory Units and Centers of the University of Ioannina.

(33) Yu, X.; Somasundaran, P. *J. Colloid Interface Sci.* **1996**, *177*, 283.

CM051450Z